Review Article | Experimental and Others

http://dx.doi.org/10.3348/kjr.2015.16.1.32
pISSN 1229-6929 · eISSN 2005-8330
Korean J Radiol 2015;16(1):32-49

Korean Journal of Radiology
KJR

Integrated Whole Body MR/PET: Where Are We?

Hye Jin Yoo, MD, PhD[1], Jae Sung Lee, PhD[2], Jeong Min Lee, MD, PhD[1, 3]

Departments of [1]Radiology and [2]Nuclear Medicine, Seoul National University Hospital, Seoul 110-744, Korea; [3]Institute of Radiation Medicine, Seoul National University College of Medicine, Seoul 110-744, Korea

Whole body integrated magnetic resonance imaging (MR)/positron emission tomography (PET) imaging systems have recently become available for clinical use and are currently being used to explore whether the combined anatomic and functional capabilities of MR imaging and the metabolic information of PET provide new insight into disease phenotypes and biology, and provide a better assessment of oncologic diseases at a lower radiation dose than a CT. This review provides an overview of the technical background of combined MR/PET systems, a discussion of the potential advantages and technical challenges of hybrid MR/PET instrumentation, as well as collection of possible solutions. Various early clinical applications of integrated MR/PET are also addressed. Finally, the workflow issues of integrated MR/PET, including maximizing diagnostic information while minimizing acquisition time are discussed.

Index terms: *MR/PET; Hybrid imaging; Positron emission tomography; Magnetic resonance imaging*

INTRODUCTION

An integrated magnetic resonance imaging (MR)/positron emission tomography (PET) system can combine functional data at the molecular level provided by PET as well as the anatomical and functional information provided by MR imaging (1-11). MR/PET is expected to show distinct advantages over PET/CT for clinical applications in which MR is known to be superior to CT, as MR imaging can offer superior soft-tissue contrast and thus allow better anatomical visualization of soft tissue and bony structures compared to that of CT. Therefore, MR/PET may be preferable when imaging the brain, head and neck, abdominal organs, pelvic organs, heart, and musculoskeletal system (2, 3, 12-18). MR/PET has gained much scientific interest as the combined anatomic and functional capabilities of MR imaging and the molecular PET information theoretically are able to provide new insight into disease phenotypes and biology, while reducing the radiation exposure to vulnerable populations such as children and women of child-bearing age (18).

In recent years, whole-body hybrid MR/PET systems, i.e., a sequential or simultaneous MR/PET system, have become commercially available and are increasingly being used in medical clinics (19). Since the recent introduction of MR/PET systems for use in clinical settings, clinical data regarding the feasibility and potential applications of integrated MR/PET have been rapidly emerging, especially in the field of oncology. Previous studies have demonstrated that the reliability of integrated MR/PET is comparable to that of PET/CT systems regarding lesion detection and anatomic allocation of abnormal findings in patients with oncologic diseases (20) and that the integrated MR/PET

Received August 6, 2014; accepted after revision September 9, 2014.

Corresponding author: Jeong Min Lee, MD, PhD, Department of Radiology and Institute of Radiation Medicine, Seoul National University College of Medicine, 101 Daehak-ro, Jongno-gu, Seoul 110-744, Korea.
• Tel: (822) 2072-3154 • Fax: (822) 743-6385
• E-mail: jmsh@snu.ac.kr

Korean Journal of Radiology
KJR

showed a 97.4% agreement rate through intra-subject comparison with PET/CT in 80 oncology patients (21).

Despite the fact that simultaneous MR/PET imaging is an intriguing research tool, its clinical applications are currently uncertain (22). Furthermore, in order to compete with PET/CT, image acquisition times should ideally be limited to 30 minutes. In PET/CT, the options for various CT protocols are limited; however, the MR imaging portion of MR/PET imaging can vary depending on the MR pulse sequences chosen and can thus easily exceed 30 minutes (22). In this report, we briefly address the technical aspects of whole-body integrated MR/PET systems, review the early clinical experience with a focus on oncologic applications of whole-body integrated MR/PET, and suggest potential new roles for integrated MR/PET imaging.

Technical Challenges of MR/PET Compared with PET/CT

Sequential vs. Simultaneous MR/PET Approaches

Two main strategies have emerged for combining PET and MR imaging in the same patient. The strategies can be distinguished by the temporal association between the two scans; they are either acquired sequentially or simultaneously (22). The sequential MR/PET is the most straightforward approach in which two, completely independent, PET and MRI systems are performed sequentially. When using this system, the patient is delivered from one scanner to the other by means of a mobile bed, i.e., a "shuttle", in order to keep the patient on a single bed for both scans (9, 23). The sequential strategy can be further divided into two categories: systems in one room with the patient shuttled between both devices with back-to-back configurations (for example, the Ingenuity TF system developed by Philips Healthcare, Best, the Netherlands); and systems in adjacent rooms with the shuttle links system going through a door (for example, the PET/CT + MR Trimodality Imaging system developed by GE Healthcare, Waukesha, WI, USA) (23, 24). The advantage of this latter design is that the two imaging units can be operated separately in times of a high workload (23, 24). It can also use its own state-of-the art time-of-flight (TOF) PET scanner. However, simultaneous data acquisition is not possible using this approach. Co-registration of the PET and MR images is still problematic because the pose of the body and the position of the internal organs can change substantially between the imaging on the two scanners due to transit (24).

In recent years, a fully integrated whole-body MR/PET scanner (Biograph mMR developed by Siemens Healthcare, Erlangen, Germany) has been introduced. When using this system, the PET detector is placed in the space between the gradient coils and the radiofrequency body coil, using the additional bore space of a more advanced gradient design (4, 23, 25). The resulting single gantry with two scanners allows for the simultaneous acquisition of whole-body PET and MR data, providing a more accurate anatomic and temporal registration of the MR and PET signals. Furthermore, the examination time can be reduced and a large room for two separated scanners is not required.

Technical Challenges

Several technical obstacles had to be overcome in order to achieve simultaneous imaging with PET and MR scanners, including the interference between the PET and MRI imaging systems, the limited bore-size of the magnets, MR-based attenuation correction of the PET data, and correction of the PET data for motion during the scan. The first simultaneously acquired MR/PET images relied on the use of a magnet field-insensitive PET detector, an avalanche Photodiode (APD)-based PET detector, and new gradient designs with the larger (70 cm) bore diameters of MR magnets. Although the quantum efficiency is higher and the devices are more compact in APDs-PET detectors, the reduced signal-to-noise ratio (SNR) makes it impossible to implement TOF technology. A new generation of solid-state photosensors has been developed which overcome the limitations of APDs (24). Silicon Photomultiplier (SiPM)-based systems offer a higher gain, higher SNR, and the faster temporal resolution required for TOF applications (24). Several research groups have been active in building SiPM-based, MR-compatible PET systems (24). Another technical issue occurred when the PET system interfered with MR imaging. PET detectors inserted into the MRI scanner can negatively affect all of the MR parameters due to electromagnetic interference (4, 24). To minimize radiofrequency (RF) interference caused by PET electronics, RF shielding is used with walled copper screens, although this can decrease the SNR. To date, the approaches for RF shielding used in the MR/PET system vary from no shielding at all to complex shield geometries (24). Still, many studies are being performed to assess the impact of various shielding strategies. A larger bore MR imaging system was also challenging because the gradient systems pay a steep

price and performance penalty for its increased size (4, 23, 25). Currently commercially available MR imaging units have a larger bore diameter (70 cm) sufficient for PET detectors and the newer gradient designs allow for peak performance with larger bore diameters. With these technical developments regarding RF shielding, MR magnets, gradient coils, and PET detectors, the simultaneous acquisition of PET and MRI images is possible in a fully integrated whole-body MR/PET scanner.

Attenuation Correction in MR/PET

Because PET image reconstruction mainly relies on the coincidental detection of emitted photon pairs, the loss of photons through body matter causes a significant attenuation of the PET signal from deep structures. In addition, the modern PET scanners that collect photon pairs in the 3D mode without the use of inter-plane septa, result in a large fraction of Compton scattering. Therefore, the attenuation and scatter corrections are essential processes for the generation of artifact-free, quantitatively accurate PET images (26, 27). In conventional, stand-alone PET scanners, the effect of photon attenuation is directly measured by the transmission scans using external radionuclide sources such as $^{68}Ge/^{68}Ga$ and ^{137}Cs. The attenuation map derived from the transmission scan is also used for scatter correction and is necessary in order to preserve image contrast (28). In combined PET/CT scanners, the PET attenuation map for 511 keV photons is derived from X-ray CT images using a piece-wise, linear transformation function (29, 30). The scan time required for whole-body PET as well as its image quality has been remarkably improved by the CT-based PET attenuation correction because it has eliminated the lengthy PET transmission scan while providing essentially noiseless attenuation correction factors (31).

However, the MRI-based PET attenuation correction is technically challenging because MR image intensity is largely determined by the tissue's hydrogen density and relaxation properties. Moreover, the presence of MR RF coils, serious attenuators of 511 keV photons, in the MR images, and truncation artifacts in PET reconstruction caused by the limited MR field-of-view (32-34), are other challenges faced by MRI-based attenuation corrections.

Several template-guided (or atlas-based) and segmentation-based methods have been suggested for MRI-based attenuation correction (35-37). In template-guided attenuation correction approaches, the template of the PET attenuation map is transformed into an individual space using the transformation parameters obtained by the nonlinear registration of individual and template MR or the emission PET data (35, 36). The template-guided attenuation correction has been well established, especially for brain PET data. Although incorporation of bone information into the attenuation map is relatively easy when using the template-guided method, the routine use of this approach for clinical MR/PET data is limited because of the potential risk of a nonlinear registration error, mainly caused by large, inter-patient anatomic variations (15). The combined approach based on template-guided and pattern recognition was also suggested, and provides better overall PET quantification accuracy than the basic MRI segmentation approach (38, 39). In the segmentation-based, attenuation correction approaches, which are mostly used in commercially available clinical MR/PET systems, individual MR images are segmented into several tissue classes and known attenuation coefficients are assigned to them (40-42). For whole-body or torso MR/PET studies, three (soft-tissue, lung, and air) or four (water, fat, lung, and air) tissue classes are automatically segmented without considering the bone tissue. For the four-class tissue segmentation, a Dixon MRI sequence is used for distinguishing water and fat tissue (Fig. 1) (40). Ignoring the bone tissue results in a considerable PET quantification error in bone lesions, but does not seem to change the clinical interpretation (43-45). A comparative study of the MR/PET segmentation-based attenuation correction methods suggested that the inclusion of both the bone and fat segments reduces the bias in PET standardized uptake value (SUV) (44).

Inclusion of bone segments in head datasets is essential, as the brain is surrounded by cortical bones (13, 46). Failure to account for bone attenuation in brain PETs introduces a spatially variable bias, which is highest in the other cortical structures and lower in the central brain (13). The currently used method for cortical-bone segmentation in head MRI is the ultrashort echo time (UTE) sequence which is specially designed to visualize tissue with a short T2 relaxation time (41). With this method, MR images acquired at two different echo times, i.e., ultra-short and typical times, are compared in order to identify the bone regions (Fig. 2). Initial versions of the UTE sequence sometimes yield errors in determining the boundary between soft tissue and air and in classifying the ventricle as cerebrospinal fluid (45, 47, 48). Therefore, it is necessary to continue to

Korean Journal of Radiology
KJR

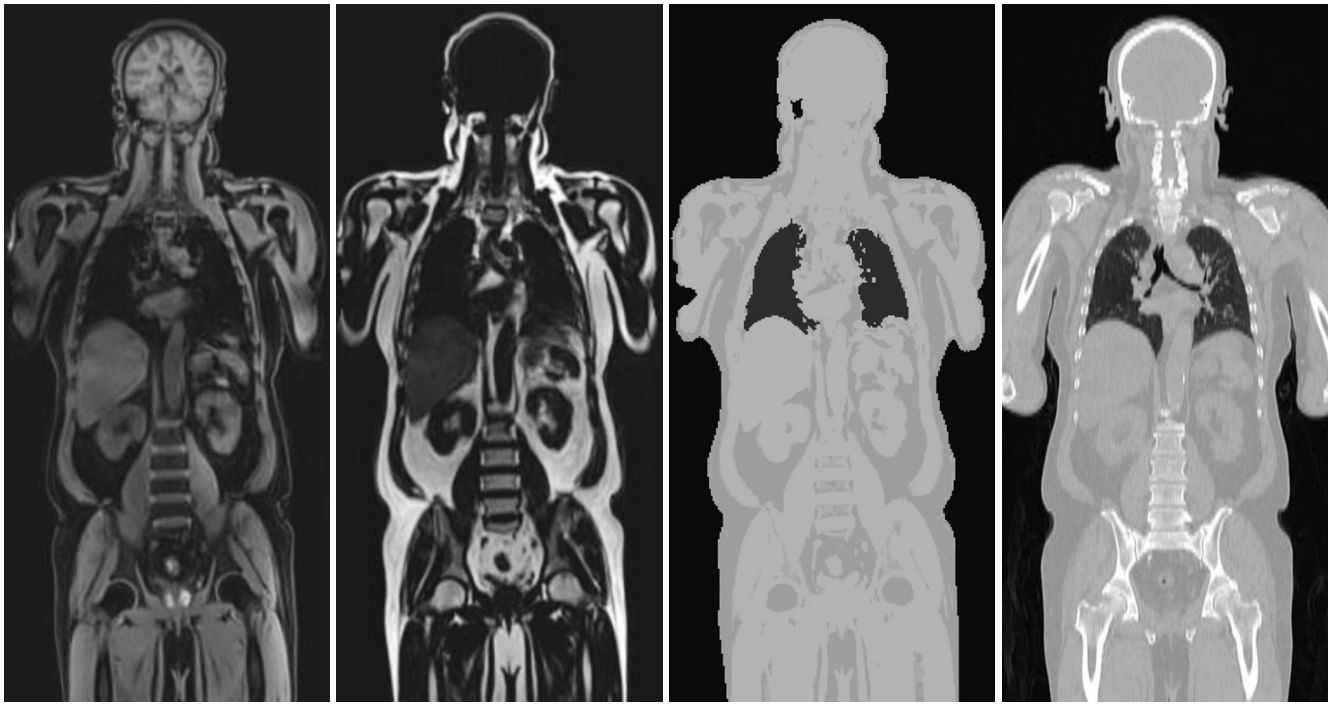

Fig. 1. Dixon MRI-based attenuation correction.
Dixon water **(A)** and fat **(B)** images. **C.** MRI-based attenuation map generated by combining water and fat images. **D.** CT of same patient.

optimize and further develop MR pulse sequences and image segmentation methods in order to enhance the generation of the PET attenuation map.

In addition, joint estimation of the radioactivity and attenuation from the emission PET data using a constrained maximum likelihood approach (Maximum Likelihood reconstruction of Attenuation and Activity; MLAA) is an alternative method for generating a PET attenuation map (49). Incorporation of the TOF information in the MLAA improves the robustness of the joint estimation (50). TOF reconstruction is also more robust than non-TOF reconstruction when the attenuation correction is not accurate (51, 52). It is, therefore, expected that the MR/PET scanners with TOF measurement capabilities will provide improved PET attenuation correction.

Workflow Considerations in MR/PET Imaging

The current fully integrated whole-body MR/PET imaging consists of two parts, i.e., whole-body MR/PET and dedicated MRI (Fig. 3). Whole-body MR/PET requires multiple bed positions due to the limited transaxial range of a PET detector (25.8 cm coverage along the z-axis) in current integrated MR/PET systems. At each bed position, PET imaging is acquired within 2–5 minutes, and the simultaneous MR data acquisition must fit into this time frame. The MRI sequences include the Dixon-based MR sequence for attenuation correction, which takes 19 seconds per bed position, and the subsequent, two or three diagnostic MR pulse sequences which include half-Fourier acquisition single-shot turbo-spin-echo, short-tau inversion-recovery (STIR) T2-weighted sequences, 3D volumetric interpolated breath-hold examination (VIBE), or turbo spin echo T1-weighted images. The whole-body examination usually requires 20–30 minutes for completion. After completion of a whole-body scan, dedicated MR imaging confined to one bed position is started with or without simultaneous PET data acquisition. The dedicated MR imaging includes standard anatomic sequences and multiparametric MR sequences such as diffusion-weighted imaging (DWI), perfusion-weighted imaging (PWI), and dynamic contrast-enhanced (DCE) MR sequences, depending on the diagnostic purposes. For clinical practice, whole-body MR/PET should have a reasonable scan time, usually not exceeding 60 minutes, and should provide maximum diagnostic information, giving it added clinical value to that of PET/CT or MRI alone. Further investigation is needed to optimize and tailor the MR imaging protocols according to clinical study purposes.

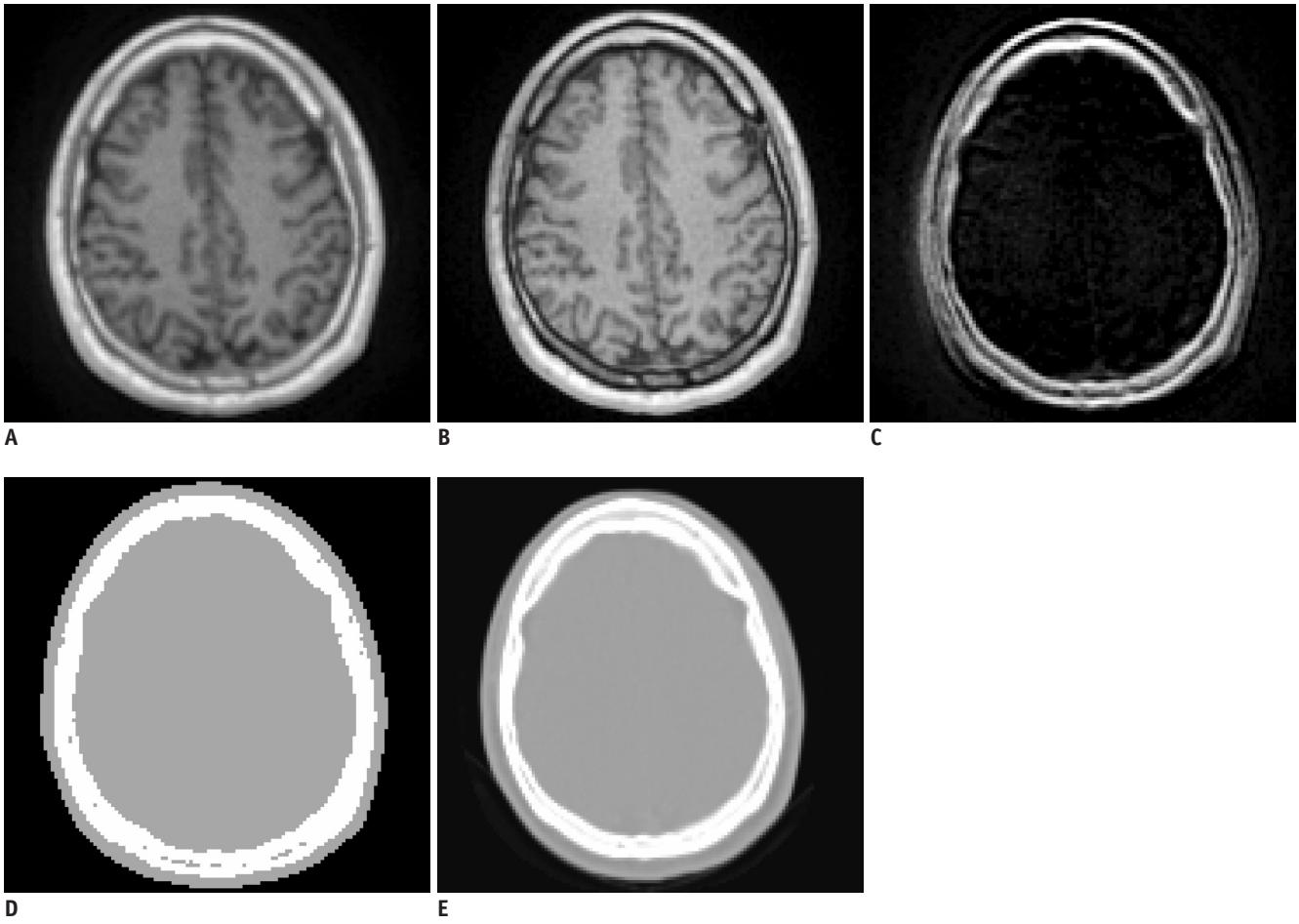

Fig. 2. Ultrashort echo time (UTE) MRI-based attenuation correction.
MR images acquired at first **(A)** and second **(B)** echo times (echo time = 0.07 ms and 2.46 ms, respectively). **C.** Differential image of **A** and **B**. **D.** UTE-based attenuation map. **E.** CT of same patient.

	Whole body MR/PET				Dedicated MR/PET	
2–5 min/bed	PET		AC	Diagnostic MR pulse sequences		
	PET		AC	Diagnostic MR pulse sequences		
	PET		AC	Diagnostic MR pulse sequences		
	PET		AC	Diagnostic MR pulse sequences	PET	Anatomic MR sequences Multiparametric MR Other functional MR
	PET		AC	Diagnostic MR pulse sequences		
Time	25–30 min				60 min	

Fig. 3. Whole-body acquisition protocol of MR/PET in oncology patients, which consists of whole-body and dedicated MR/PET.
Diagnostic MR pulse sequences in whole-body MR/PET include half-Fourier acquisition single shot turbo spin echo, short-tau inversion recovery T2-weighted sequences, three-dimensional volumetric interpolated breath-held examination or turbo spin echo T1-weighted images. On dedicated MR imaging, variable pulse sequences were used according to diagnostic purpose and specific body part. AC = attenuation correction, MR/PET = magnetic resonance imaging/positron emission tomography

Korean Journal of Radiology
KJR

MR/PET Imaging for Oncologic Diseases

PET/CT using ^{18}F-fluorodeoxyglucose (FDG) serves as a diagnostic, prognostic, and intermediate endpoint biomarker in cancer patients and is now recognized as ane important imaging tools in the management of oncology patients (18, 53). Although the diagnostic accuracy of PET/CT for evaluating various malignant tumors is high, one of the major potential advantages of integrated MR/PET imaging systems compared with PET/CT is its ability to provide improved clinical assessments of cancers in tissue that may be anatomically better characterized by MR imaging than by CT. This includes cancers of the brain, head and neck, breast, liver, pancreas, musculoskeletal system, and the prostate gland (18). Furthermore, considering the multiparameteric capability of MR for the functional assessment of biological phenomena, integrated MR/PET is a promising new imaging tool, especially for the diagnostic work-up of patients with cancer, as it delivers a sensitive whole-body survey, combining molecular, functional, and anatomical data, in only one examination (54). However, in order to increase the clinical use of MR/PET, there are still several obstacles to overcome, including the high cost of MR/PET and the limited patient throughput due to acquisition of the anatomical and functional information of MR.

TNM Staging

The staging workup evaluating the tumor extent and infiltration of adjacent organs is important for choosing the optimal treatment and for estimating the patient prognosis. By combining MR imaging and PET imaging, integrated MR/PET can improve the diagnostic accuracy in oncology staging. MR imaging not only gives a detailed anatomic evaluation of soft tissue but also provides opportunities to evaluate tissue function using multiparametric MR sequences, such as DWI, PWI, and MR spectroscopy (MRS) (55-57). Improvement of diagnostic accuracy of oncologic staging using integrated MR/PET might directly affect patient care by identifying the most suitable therapy.

T-Staging

The assessment of the exact tumor localization, tumor invasion into adjacent organs, and neurovascular structures

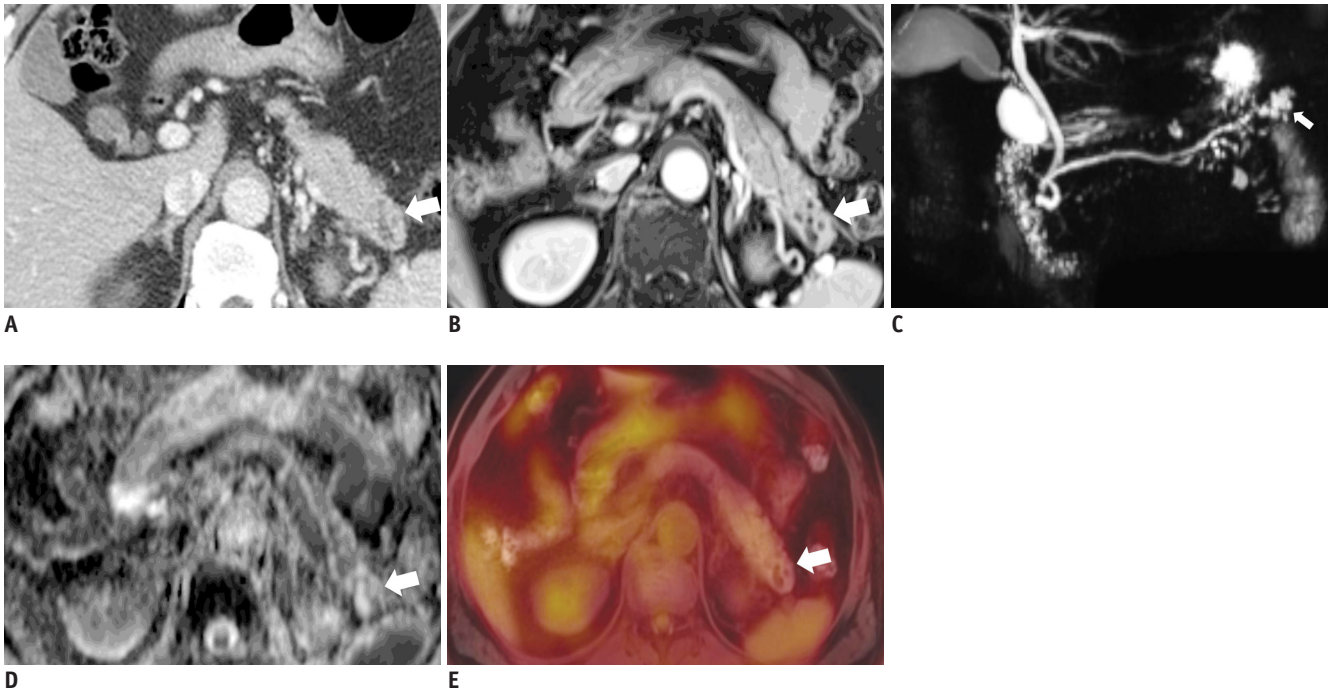

Fig. 4. 63-year-old male had pancreatic mass.
A. Axial CT image showed 2.5-cm, low-attenuated mass with heterogeneous enhancement (arrow) in pancreas tail, which was indeterminate finding. **B.** Axial, post-contrast, T1-weighted image demonstrated conglomerated cystic mass (arrow) with septal enhancement. **C.** MR cholangiopancreaticography also showed conglomerated cystic mass (arrow) in pancreas tail. **D.** ADC map showed no diffusion restriction in mass (arrow). **E.** Fused FDG-MR/PET image showed no FDG uptake in mass (arrow). Anatomical MR images **(B, C)** were helpful for characterizing mass, and functional images **(D, E)** suggested that mass was benign lesion. Mass was resected and confirmed as serous cystadenoma. ADC = apparent diffusion coefficient, FDG = fluorodeoxyglucose, MR/PET = magnetic resonance imaging/positron emission tomography

(T-staging) relies primarily on the information provided by the high spatial resolution of MR imaging. Therefore, integrated MR/PET may be superior to PET/CT for all tumors in which MR imaging is known to be superior to CT due to its high soft-tissue contrast, including brain tumors (58), head and neck cancer (59-61), gynecologic and intra-abdominal tumors (Fig. 4) (5, 12, 20, 62-65), and soft-tissue sarcomas (16, 66).

In a recent previous study by Sun et al. (63), good anatomical agreement between PET and T2-weighted MR imaging (T2WI) and functional volume concordance between PET and DWI were seen in MR/PET in cervical cancer, which would benefit clinical decision-making in preoperative staging. In addition, recent studies have reported encouraging results using co-registered choline PET/CT and T2WI/DWI MR imaging or fused acetate MR/PET for primary prostate cancer detection and staging (67, 68). Integrated imaging may overcome the known limitations of morphologic MR imaging or MR spectroscopy with choline in the localization of prostate cancer (55, 64). A recent study by Takei et al. (69) demonstrated that multimodality multiparametric choline MR/PET was helpful for determining the biopsy target site in previously biopsy-negative, primary prostate cancer, which was mainly due to the superior soft-tissue contrast of MR imaging. Moreover, Afshar-Oromieh et al. (70) introduced the new radiotracer, Ga-labelled prostate-specific membrane antigen, which is more selectively accumulated in prostate cancer, as seen in integrated MR/PET, in order to improve the detection of prostate cancer with less radiation exposure.

For intraabdominal malignancy, Gaertner et al. (65) evaluated the feasibility of simultaneous ^{68}Ga-DOTATOC MR/PET in 24 patients with neuroendocrine tumors. In the study, they reported that anatomical correlates for focal PET uptake lesions could more often be delineated using MR Dixon images compared with low-dose CT and the difference was significant ($p < 0.01$), although there was no significant difference in the co-registration of functional and morphologic data ($p = 0.10$) and the lesion conspicuity was significantly higher on PET/CT ($p = 0.01$). For primary hepatic tumors or hepatocellular carcinoma, data regarding the diagnostic performance of integrated MR/PET for the detection of tumors are still lacking. If dedicated MR imaging using a liver-specific contrast agent, such as gadoxetic acid, and functional MR techniques, such as DWI or PWI, can be applied to integrated MR/PET imaging, MR/PET may be advantageous for the diagnosis of hepatocellular carcinoma (17).

Another important potential indication for the use of MR/PET is soft-tissue sarcoma, as MR imaging with high soft-tissue contrast has a key role in the staging and evaluation of the disease (16). Compared to stand-alone MR imaging, the contribution of MR/PET in the diagnosis of soft-tissue sarcomas is expected in the differentiation between malignant and benign soft-tissue masses as well as in the preoperative surgical planning, as FDG-PET can help to determine a safe, tumor-free surgical margin. However, no preliminary study regarding the assessment of soft-tissue sarcoma using integrated MR/PET is currently available except for one case report. Schuler et al. (71) demonstrated that in large and heterogeneous tumors, MR/PET can help guide the tumor biopsy or judge the grading of the tumor, both of which are important in order to determine the optimal therapeutic options.

In breast imaging, MR mammography has been widely used for the primary tumor detection and characterization of breast lesions (17). However, it lacks specificity and is strongly dependent on the reader's degree of clinical experience (17). By combining the PET data, MR/PET can be expected to improve its diagnostic accuracy in the evaluation of breast cancer. However, there has been no proven diagnostic benefit from the software-based fusion of PET and MR imaging or integrated MR/PET because equivocal, small lesions have often demonstrated a low degree of FDG uptake, even when malignant (17, 72). MR/PET might be helpful for estimating the prognosis of breast cancer patients as it is known that higher SUVs in PET imaging indicate a poorer clinical prognosis and for evaluating recurrent or metastatic breast cancer (17, 72).

For head and neck cancer, Platzek et al. (61) reported promising results of sequential MR/PET for the detection of primary tumors compared with PET alone or MRI alone: more primary tumors were detected using MR/PET (n = 17 of the 20 patients) compared with PET-only datasets (n = 16/20) or MRI-only datasets (n = 14/20), respectively. However, another prospective study by Kubiessa et al. (73) showed that integrated MR/PET of patients with head and neck cancer yielded a sensitivity of 80.5% and a specificity of 88.2%, similar to that of PET/CT in which the corresponding values were 82.7% and 87.3%.

These initial clinical experiences using integrated MR/PET show promising results indicating that MR/PET is feasible for evaluation of various oncologic diseases, although further prospective clinical studies with larger patient

Korean Journal of Radiology
KJR

populations are warranted.

N-Staging

For the evaluation of locoregional lymph-node metastasis, cross-sectional imaging modalities, including CT and MR imaging, are dependent mainly on the size and shape of lymph nodes in order to differentiate benign from malignant lymph nodes, and thus resulting in the relatively low accuracy in N-staging (60). The addition of the metabolic information of PET imaging has been shown to significantly improve the diagnostic accuracy of N-staging compared with that of CT (74). As MR imaging also relies on the morphologic criteria, similar to those of CT, for the assessment of lymph-node metastasis, the simple combination of PET and MR imaging is not expected to have advantages over PET/CT for N-staging (1, 5, 17). Another problem of N-staging is the detection of microscopic metastasis in lymph nodes, as the spatial resolution of PET imaging is limited for detecting it and lymph nodes with micrometastasis often have a morphologically normal shape and size without significant FDG uptake. To date, there are only a few clinical reports regarding the diagnostic performance of MR/PET in N-staging. Recently, Kohan et al. (75) performed a study in 11 patients with lung cancer in order to evaluate the performance of sequential MR/PET for detecting lymph-node metastasis. They reported that the overall interobserver agreement was high (κ = 0.86) for PET/CT and substantial (κ = 0.70) for MR/PET, although the diagnostic accuracy of MR/PET (0.77) for N-staging was slightly less than that of PET/CT (0.80), although the difference was not statistically significant. Considering the previous studies evaluating the additional values of STIR and DWI in the N-staging of lung cancer patients, further studies using multiparametric MRI sequences should be performed in order to improve the diagnostic performance of MR/PET in the detection of metastasized lymph nodes

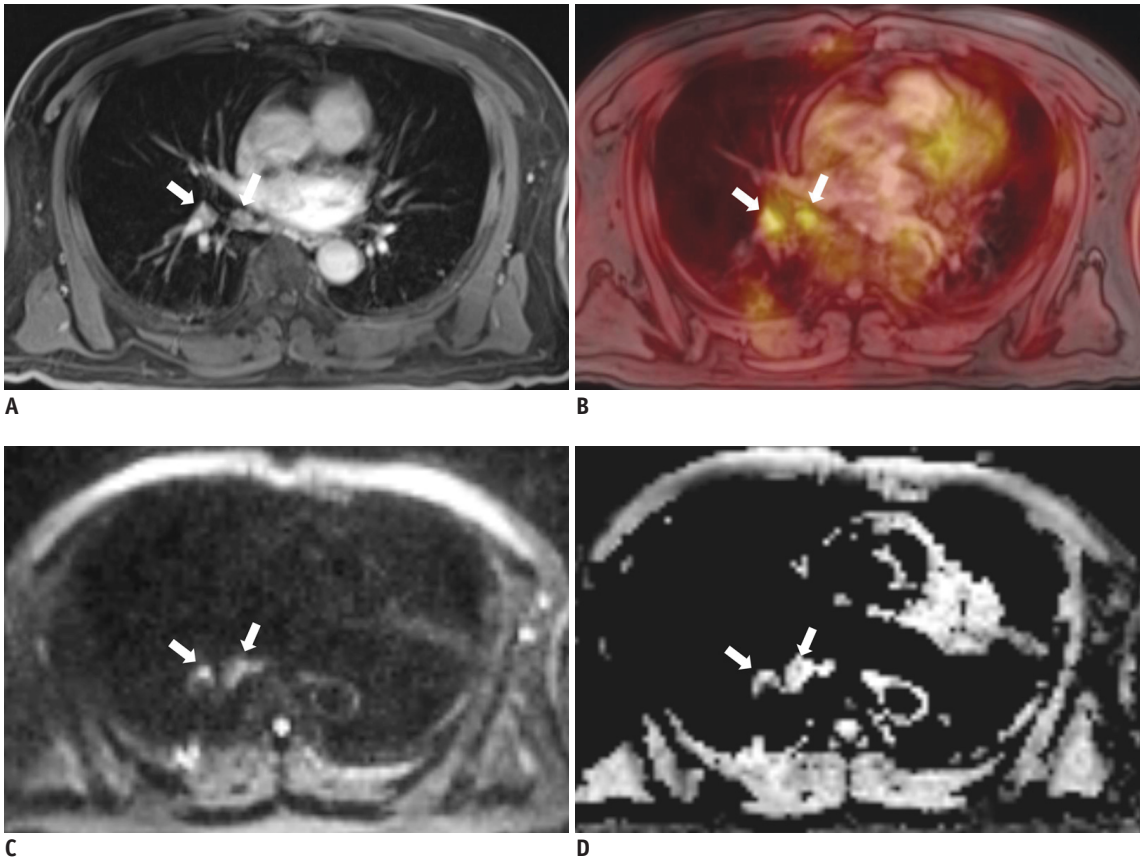

Fig. 5. 66-year-old man with 3.7-cm lung mass (not shown) in right lower lobe.
A. Axial, post-contrast, three-dimensional volumetric interpolated breath-hold examination image showed two small right interlobar lymph nodes (arrows). **B.** Axial fused FDG-MR/PET image showed increased FDG uptake in interlobar nodes (SUVmax: 4.4 and 3.8). Axial, DWI (b = 400) **(C)** and ADC map showed diffusion restriction in two lymph nodes **(D)**. Concordant findings of right interlobar lymph nodes on ADC map and on fused MR/PET image increased our confidence in reporting right interlobar lymph-node metastasis, and pathology results confirmed right interlobar lymph-node metastasis. ADC = apparent diffusion coefficient, DWI = diffusion-weighted image, FDG = fluorodeoxyglucose, MR/PET = magnetic resonance imaging/positron emission tomography, SUVmax = maximum standardized uptake value

(Fig. 5). The additional use of an MR contrast agent specific for the reticuloendothelial system, such as ultra-small iron oxide particles (USPIO), or a new radiotracer will need to be considered in future research studies (1, 5, 76). Thorek et al. (76) presented a multimodal nanoparticle, ^{89}Zr-ferumoxytol, for the enhanced detection of lymph nodes

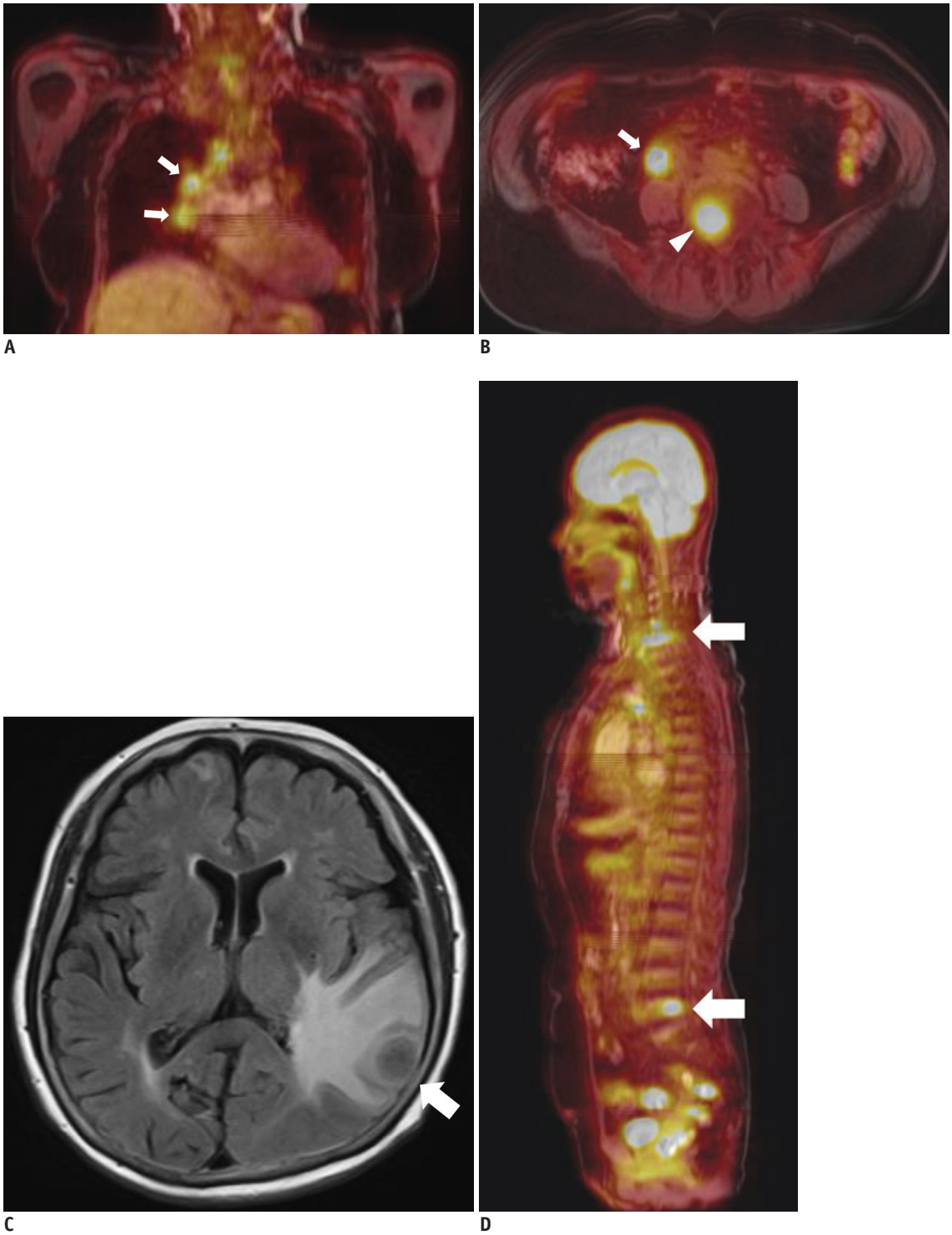

Fig. 6. 63-year-old male had colon cancer with brain, lung, and mediastinal lymph node (LN) metastasis.
A. Coronal fused FDG-MR/PET image showed mediastinal LNs (arrows) with increased FDG uptake. **B.** Axial fused FDG-MR/PET image showed metastatic retroperitoneal LN (arrow) and metastatic bone lesion at L5 vertebral body (arrowhead). **C.** FLAIR image demonstrates brain metastasis in left temporal lobe (arrow). **D.** Reconstructed sagittal fused FDG-MR/PET image showed bone metastasis in cervical and lumbar spine (arrows). FDG = fluorodeoxyglucose, FLAIR = fluid attenuated inversion recovery, MR/PET = magnetic resonance imaging/positron emission tomography

Korean Journal of Radiology
KJR

(LNs) using MR/PET in preclinical disease models. Their work showed that MR/PET could be successfully used to localize the axillary and prostate draining lymphatics using radiolabeled nanoparticles.

M-Staging

MR imaging has been reported to be of higher accuracy than PET/CT when assessing the liver and bone (Fig. 6) for distant metastases (1, 5, 45, 77-82). In a recent study (45) which compared PET/CT scanning and a subsequent MR/PET with an unenhanced coronal T1-weighted turbo spin-echo (T1WI-TSE) sequence for the analysis of bone lesions in 119 patients with primary malignancies, the anatomic delineation and allocation of bone lesions was significantly superior with T1WI-TSE MRI compared to CT or T1-weighted VIBE Dixon MRI. No significant difference in the correct classification of malignant bone lesions was found among the image sets. These results suggest that MR/PET, with the diagnostic T1WI-TSE sequence, could be useful for diagnosing primary bone tumors, early bone marrow infiltration, and tumors with low avidity to FDG. Underestimation of FDG uptake in bone was also found on MR/PET due to an under-correction of cortical bone when creating an MR-based attenuation map, although there was a highly significant correlation between the SUVs for MR/PET and PET/CT ($p < 0.0001$) (45).

Despite the fact that reliable data regarding the diagnostic performance of integrated MR/PET for detecting liver or brain metastasis is still lacking, it is obvious that liver or brain metastasis (Fig. 6) will also be detected more easily using MR/PET imaging. Previous studies conducted using retrospective fusion images of PET/CT and MRI suggested that the sensitivity of MR/PET imaging for the detection of liver metastases is higher than that of PET/CT due to the high soft-tissue contrast of MR imaging (62, 82, 83). For brain metastasis, while FDG PET detected only 61% of the metastases detected on MRI alone due to the high physiologic FDG uptake in brain tissue, adding PET data to brain MRI was shown to be valuable for the specification of morphologically indistinguishable, contrast-enhancing lesions found on MRI (17, 84). Integrated MR/PET using DWI and DCE MRI with an organ-specific contrast agent could improve the accuracy for the detection of liver or brain metastasis (54).

To detect lung metastasis, CT is still the standard and best imaging modality due to its higher sensitivity in the relevant tissue (85). In a recent study (86), which assessed the diagnostic sensitivity of integrated MR/PET using a radial, T1-weighted, gradient-echo (radial VIBE Siemens Healthcare, Erlangen, Germany) MR sequence for

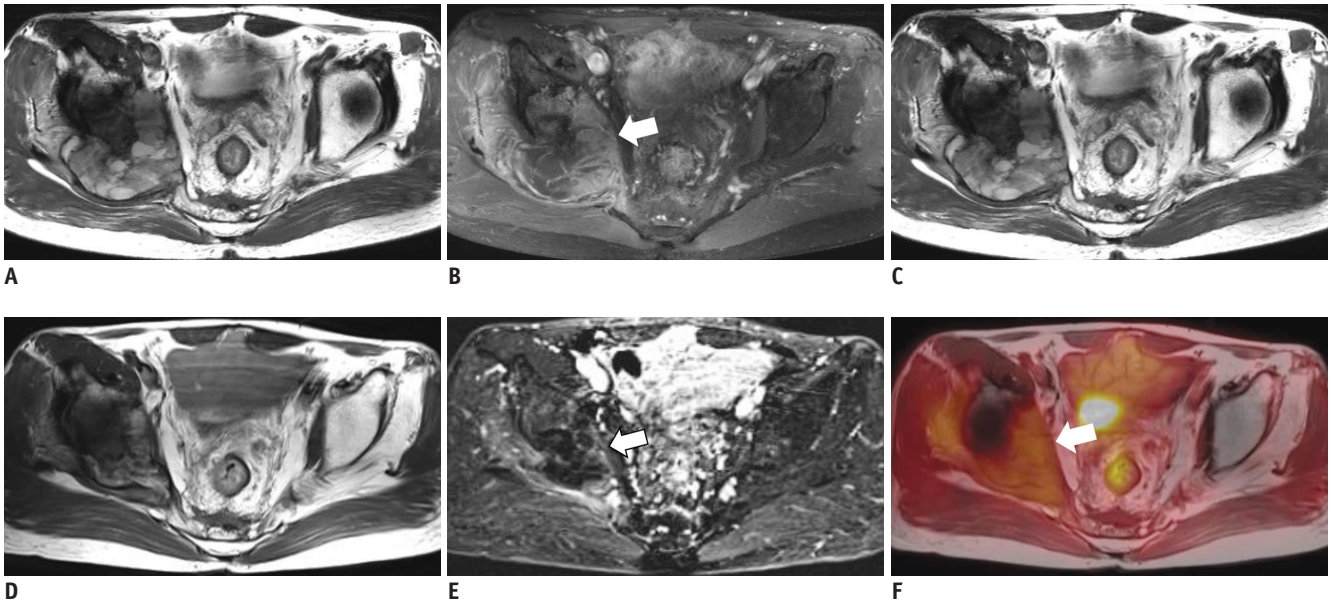

Fig. 7. 53-year-old male with radiation-induced osteosarcoma in right ilium before (A-C) and after (D-F) chemotherapy.
A. Axial, T2-weighted MR image showed heterogeneous, T2 hyperintense soft-tissue mass in right ilium. **B.** Axial, post-contrast, T1-weighted MR image showed soft-tissue enhancement (arrow) with central non-enhancement before chemotherapy. **C.** Axial PET-CT image demonstrated increased FDG uptake (SUVmax = 21.84) in corresponding lesion. **D.** Axial, T2-weighted MR image obtained after chemotherapy shows decrease in tumor size. **E.** Axial, post-contrast, T1-weighted MR image obtained after chemotherapy shows decrease in area of soft-tissue enhancement (arrow). **F.** Corresponding to fused FDG-MR/PET image obtained after chemotherapy and which showed no pathological FDG uptake (SUVmax = 2.23). FDG = fluorodeoxyglucose, MR/PET = magnetic resonance imaging/positron emission tomography, SUVmax = maximum standardized uptake value

the detection of lung nodules, the sensitivity of MR/PET was 70.3% for all nodules, 95.6% for FDG-avid nodules, and 88.6% for nodules 0.5-cm or larger in diameter. However, as MR/PET was still limited for the detection of small (< 0.5-cm) and non-FDG avid lung nodules, further investigation into more successful MR sequences and techniques is needed.

Response Evaluation

Until now, treatment response has been primarily assessed by anatomical imaging based on the Response Evaluation Criteria in Solid Tumors criteria (87). Tumor sizes are best measured using CT or MR imaging. However, there have been limitations regarding the evaluation of the metabolic response to treatment when using only morphologic measurements. In recent years, PET/CT has been thought to be an essential imaging modality for response evaluation and therapy monitoring in various tumors (87). DWI is also being increasingly used to assess tumor response as early changes in diffusion restriction can reflect tumor cellularity, and which can be correlated with the response to therapy accordingly (2, 88, 89). Therefore, adding functional information obtained on PET and DWI to conventional MR imaging will significantly improve diagnostic accuracy when assessing the therapeutic response (1, 6, 16). In addition, adding information regarding tissue perfusion obtained by incorporating dynamic contrast-enhanced MR imaging, and the level of oxygen saturation obtained from blood oxygen level-dependent MR imaging measurements could lead to an improved ability to distinguish specific biologic tumor compartments, and thus potentially leading to more informed therapy decisions (56).

Moreover, MR/PET could provide the information regarding not only the treatment response but also the restaging for surgical resection after neoadjuvant treatment in a single session (Figs. 7, 8). Currently, there are only a few reports that assess the potential benefit of MR/PET in the treatment

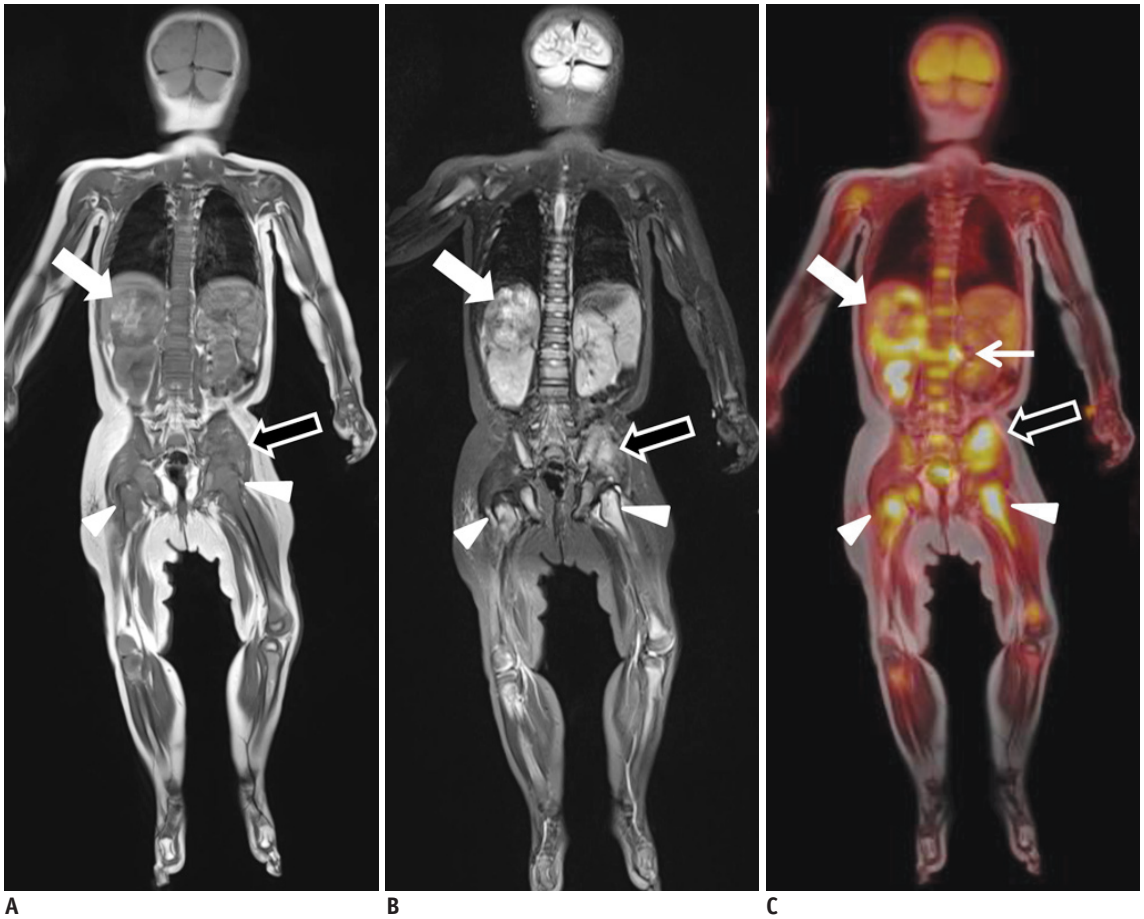

Fig. 8. One-year-old male with neuroblastoma.
Coronal, T1-weighted image **(A)** and coronal STIR T2-weighted sequences image **(B)** showed multiple, metastatic tumors in right adrenal gland (white arrow), left ilium (black arrow), and proximal metaphysis of both femora (arrowheads). **C.** Coronal FDG-MR/PET image demonstrated strong FDG uptake in lesions. Thin arrow shows multiple spine metastases. FDG = fluorodeoxyglucose, MR/PET = magnetic resonance imaging/positron emission tomography, STIR = short-tau inversion recovery

Korean Journal of Radiology
KJR

response evaluation. Platzek et al. (90) evaluated the feasibility of sequential MR/PET for the therapy response evaluation of malignant lymphoma in nine patients. They showed excellent interobserver agreement regarding the Ann Arbor stage ($\kappa = 0.97$) and good interobserver agreement regarding the image quality ($\kappa = 0.41$), thus suggesting that FDG-MR/PET is a reliable imaging method. Schuler et al. (71) reported a case of rhabdomyosarcoma for which MR/PET was used to guide neoadjuvant treatment. They were able to determine whether neoadjuvant chemotherapy was effective after the response evaluation made with MR/PET, and then could perform curable resection at the optimal time. This case demonstrates that MR/PET could be a valuable method for solving clinical problems. Based on these reports, MR/PET is expected to offer a great opportunity for tumor-response evaluation and treatment monitoring. However, both PET and DWI are weak in their ability to differentiate viable tumor from inflammation/granulation tissue after neoadjuvant treatment, although for different reasons. The simultaneous acquisition of PET and MR images may be complementary to each other. The addition of a functional component, such as perfusion MR, could help detect early responders in patients undergoing neoadjuvant therapy, giving meaningful information to determine whether a further chemotherapy cycle is needed. In addition, MR/PET can provide additional meaningful information regarding the decision-making process for clinicians, and which will be advantageous for patients who require neoadjuvant chemotherapy or radiation therapy.

Pediatric Oncology

In children, reduced radiation exposure is an important issue in determining the optimal imaging modality (91). MR/PET can minimize radiation exposure and offers a one-stop-shop diagnostic procedure that replaces the previously required multiple examinations, decreasing the length of the diagnostic period before the start of treatment (Fig. 8). Hirsch et al. (92) reported their experience using MR/PET in 15 children, finding that the effective dose of a MR/PET scan was only approximately 20% of the equivalent PET/CT examination. A lower radiation dose is important for those young patients undergoing repeated imaging and having potentially curable disease. The PET component was helpful for the detection of lymph nodes that were morphologically of borderline size but showed increased FDG uptake (93). MR imaging demonstrated an advantage in those patients with symmetrical organ involvement, which was less certain in the interpretation of PET images. Even in solid tumors, Hirsch et al. suggested that one-stop staging using MR/PET was faster and clearer than isolated whole-body MRI. Furthermore, MR/PET was beneficial for determining the biopsy site and for treatment planning (91). Due to its minimal radiation exposure and improvement of the workflow, MR/PET will be valuable in pediatric oncology (5, 91).

Lymphoma, Multiple Myeloma, and Malignant Melanoma

Lymphoma and multiple myeloma require whole-body staging at the initial diagnosis stage in order to select the most appropriate treatment methods (16). It is also essential to assess the bone-marrow (BM) involvement of the tumors, and which can be successfully performed using whole-body MR imaging with DWI (94). There is evidence that whole-body DWI, with a sensitivity of 90% and a specificity of 94%, could be as accurate as FDG PET/CT for lymphoma staging (93, 94). The addition of DWI image significantly increases the accuracy of whole-body MRI for the primary staging of lymphoma patients, leading to a 94% concordance with the findings obtained on ^{18}F-FDG PET/CT (94). In multiple myeloma, there is a growing concern that patients may be under-staged using the classic staging system with radiography due to its low sensitivity in the detection of myeloma infiltration of the BM. There is evidence that including an MR diagnosis component to the staging system would have a significant influence on the patient prognosis and survival rates (95). Therefore, MR/PET will be a tool to achieve whole-body staging, including the BM status, in one step. For malignant melanoma, in which there is often unpredictable distant metastasis, MR/PET also has advantages for the detection of subcutaneous, bone, liver, and brain metastases (16).

Cardiac MR/PET Imaging

As MR/PET imaging could provide good spatial and temporal image co-registration, simultaneous data acquisition may provide more reliable correlative results using all of the information available from both modalities (56). Theoretically, PET provides accurate measurements of perfusion, metabolism, inflammation, innervation, and ligand binding, whereas MR provides high-resolution structural data, soft-tissue contrast, and parameters of mechanical structures such as deformation, strain, viability, and fibrosis (56). Ripa et al. (96) reported their first

experiences using the integrated MR/PET system to image the carotid arteries of six HIV-positive patients who were at an increased risk for atherosclerosis but showed no overt atherosclerosis. The image quality of the MR/PET allowed for delineation of the carotid vessel wall and quantification of FDG uptake was well correlated between the MR/PET and PET/CT. The higher soft-tissue contrast of MR imaging allowed differentiation between the carotid-artery wall and the lumen, allowing more detailed analyses compared to PET/CT (97). The authors concluded that simultaneous MR/PET is feasible for carotid imaging in patients without large atherosclerotic plaques and that FDG quantification by MR/PET is comparable to that of PET/CT. Nensa et al. (98) also assessed the feasibility of heart imaging using integrated MR/PET in 20 patients with myocardiac infarctions. Their study showed substantial agreement between PET and late gadolinium-enhanced images ($\kappa = 0.76$) and between PET and cine images ($\kappa = 0.78$). They suggested that MR/PET in cardiac imaging may add complementary information for patients with ischemic heart disease. In the future, potential applications of MR/PET in cardiac imaging may be extended to varying fields of cardiology, including coronary artery disease detection, differentiation of ischemic from non-ischemic cardiomyopathy, and assessment of myocardial viability and plaque vulnerability where values of stand-alone PET or MR imaging have been proven in previous studies (99, 100). Other potential tracers for the identification of plaque inflammation/vulnerability or neoangiogenesis in atherosclerotic lesions might enhance the diagnostic performance of cardiac MR/PET imaging (100).

MR/PET Imaging in Neurology

In neuroimaging, MR/PET has various potential applications not only for neuro-oncology (17, 58, 101, 102) but also for neurodegeneration, dementia, epilepsy, and stroke (5, 25, 102). The additional functional information could be provided by PET with various radiotracers and functional MR techniques such as PWI, DWI, and MR spectroscopy (102). Another advantage of MR/PET may be its simultaneous acquisition of PET and MR imaging as a one-stop examination, which could make it possible to visualize time-dependent biologic processes (22). Examples include functional MRI measuring the task-induced changes of the blood flow and oxygen consumption rates or measurement of the arterial input function by MRI for its use in compartment modeling in quantitative PET studies (25). MR/PET can also be used for cross-validation of methods for function imaging; for example, arterial spin labeling MR imaging can be validated by ^{15}O-H_2O PET which is the gold standard for the assessment of cerebral blood flow.

Integrated MR/PET in neuro-oncology could provide morphologic information for the exact delineation of tumors, and functional information for the differentiation of tumor tissue from radiation necrosis, therapy response assessment, and preoperative grading of tumors (5, 19, 53, 102-104). MR/PET can also be useful for the preoperative localization of seizure foci in epilepsy, and the differentiation of a penumbra from infarct tissues in ischemic/vascular disease (23). Currently, although there are only a few available studies using integrated whole-body MR/PET in neuroimaging, there are some studies using prototype hybrid MR/PET scanners. In a study by Boss et al. (105) of 10 patients with intracranial masses, simultaneous MR/PET was performed after PET/CT with either ^{11}C-methionine (glial tumors) or gallium 68 (^{68}Ga)-D-phenylalanine(1)-tyrosine(3)-octreotide (meningiomas). The tumor-to-reference count density tissue ratios exhibited excellent concordance between MR/PET and PET/CT ($R = 50.98$). Similarly, Schwenzer et al. (106) studied 50 patients with intracranial masses, head and upper neck tumors, or neurodegenerative diseases using simultaneous MR/PET with ^{11}C-methionine or ^{68}Ga-D-phenylalanine(1)-tyrosine(3)-octreotide. Arterial spin labeling and proton-spectroscopy was possible in all cases. MR/PET was comparable to PET/CT in the diagnostic image quality and tumor delineation. MR/PET also revealed a high agreement of the mean asymmetry index and the mean ratio (frontal/parieto-occipital) (106). The feasibility of diffuse tensor imaging combined with simultaneous PET imaging was assessed by Boss et al. (107) in seven volunteers and four patients with brain tumors. They found that diffusion tensor imaging could be combined with simultaneous PET data acquisition, offering additional important morphologic and functional information for treatment planning in patients with brain tumors. PWI with PET may be advantageous for assessing ischemic or vascular, neurodegenerative, and neoplastic brain disorders, although the clinical evidence regarding MR/PET neuroimaging is still limited. In the future, simultaneous acquisition of various metabolic and functional parameters may offer new opportunities for diagnosing various brain diseases.

Korean Journal of Radiology
KJR

Present and Future Applications of MR/PET Imaging

MR/PET imaging can significantly reduce the patient's radiation exposure, as MR can replace CT for attenuation correction. Therefore, MR/PET can be an alternative imaging modality for pediatric and gynecologic malignancies or for patients who require multiple PET/CT scans, such as lymphoma patients (4, 90, 92, 93). Other important immediate applications of MR/PET imaging are areas in which the superior soft-tissue contrast of MR imaging offers benefits. This is mainly relevant in oncologic applications, because combination of accurate anatomic and physiological information may also improve the accuracy of T- and M-staging of malignancies. Therefore, there are many attempts to elucidate the benefits of MR/PET in head and neck, prostate, breast, musculoskeletal, and neuroendocrine tumor imaging (2, 65, 68-70, 72, 73).

MR imaging also has further potential in functional imaging using DCE, DWI, PWI, and MRS. Preliminary studies have shown that multiparametric MR imaging used in conjunction with PET might provide a more successful approach for treatment response assessment or LN-staging, whereas a conventional imaging modality such as CT or MR imaging cannot solve the problem (1, 6, 16). Combined MR/PET might help to precisely quantify a tumor's vascular properties (assessed by functional MR methods), cell proliferation, and tumor glucose metabolism (assessed with PET) (4). With an understanding of the underlying molecular biology, combined MR/PET may highlight important biomarkers to predict and monitor the targeted treatment response. Development of new MR contrast agents such as USPIO and multiparametric MR measurements might be helpful for LN-staging where conventional imaging showed mixed sensitivity and specificity. Neuropsychiatric diseases might be a future application of simultaneous MR/PET, as advanced MR techniques may be used to study the dynamics of neurotransmission. Furthermore, advanced MR techniques have the potential to significantly improve PET data quantification when using MR-assisted motion correction and partial-volume-effect correction methods. Improved quantification with PET data may have a crucial role in cardiovascular imaging (quantification of blood flow and assessing myocardial tissue viability), neuropsychiatric disease identification (quantification of amyloid and tau-protein in Alzheimer's disease), and new drug development (assessing the pharmacokinetics and pharmacodynamics of a drug).

In the future, much effort will be needed in order to provide specific, reliable, and sensitive radiotracers and MR contrast agents for interesting new applications, especially in oncologic and neurologic imaging. Fortunately, several promising radiopharmaceuticals are being developed. Ligands for prostate-specific membrane antigens, gastrin-releasing peptide receptors, amino acid transport in the brain, and an amyloid-targeting PET probe have recently been demonstrated (22, 53, 54). With new non-FDG tracers, MR/PET will be a promising new imaging tool not only in clinical practice but also in research to identify its further advantages and applications.

REFERENCES

1. Antoch G, Bockisch A. Combined PET/MRI: a new dimension in whole-body oncology imaging? *Eur J Nucl Med Mol Imaging* 2009;36 Suppl 1:S113-S120
2. Balyasnikova S, Löfgren J, de Nijs R, Zamogilnaya Y, Højgaard L, Fischer BM. PET/MR in oncology: an introduction with focus on MR and future perspectives for hybrid imaging. *Am J Nucl Med Mol Imaging* 2012;2:458-474
3. Catalano OA, Rosen BR, Sahani DV, Hahn PF, Guimaraes AR, Vangel MG, et al. Clinical impact of PET/MR imaging in patients with cancer undergoing same-day PET/CT: initial experience in 134 patients--a hypothesis-generating exploratory study. *Radiology* 2013;269:857-869
4. Catana C, Guimaraes AR, Rosen BR. PET and MR imaging: the odd couple or a match made in heaven? *J Nucl Med* 2013;54:815-824
5. Gaertner FC, Fürst S, Schwaiger M. PET/MR: a paradigm shift. *Cancer Imaging* 2013;13:36-52
6. Herzog H. PET/MRI: challenges, solutions and perspectives. *Z Med Phys* 2012;22:281-298
7. Jadvar H, Colletti PM. Competitive advantage of PET/MRI. *Eur J Radiol* 2014;83:84-94
8. Pichler BJ, Judenhofer MS, Pfannenberg C. Multimodal imaging approaches: PET/CT and PET/MRI. *Handb Exp Pharmacol* 2008;(185 Pt 1):109-132
9. von Schulthess GK, Schlemmer HP. A look ahead: PET/MR versus PET/CT. *Eur J Nucl Med Mol Imaging* 2009;36 Suppl 1:S3-S9
10. Wehrl HF, Sauter AW, Judenhofer MS, Pichler BJ. Combined PET/MR imaging--technology and applications. *Technol Cancer Res Treat* 2010;9:5-20
11. Zaidi H, Montandon ML, Alavi A. The clinical role of fusion imaging using PET, CT, and MR imaging. *Magn Reson Imaging Clin N Am* 2010;18:133-149
12. Al-Nabhani KZ, Syed R, Michopoulou S, Alkalbani J, Afaq A, Panagiotidis E, et al. Qualitative and quantitative comparison of PET/CT and PET/MR imaging in clinical

practice. *J Nucl Med* 2014;55:88-94
13. Andersen FL, Ladefoged CN, Beyer T, Keller SH, Hansen AE, Højgaard L, et al. Combined PET/MR imaging in neurology: MR-based attenuation correction implies a strong spatial bias when ignoring bone. *Neuroimage* 2014;84:206-216
14. Bailey DL, Barthel H, Beuthin-Baumann B, Beyer T, Bisdas S, Boellaard R, et al. Combined PET/MR: Where are we now? Summary report of the second international workshop on PET/MR imaging April 8-12, 2013, Tubingen, Germany. *Mol Imaging Biol* 2014;16:295-310
15. Boss A, Stegger L, Bisdas S, Kolb A, Schwenzer N, Pfister M, et al. Feasibility of simultaneous PET/MR imaging in the head and upper neck area. *Eur Radiol* 2011;21:1439-1446
16. Buchbender C, Heusner TA, Lauenstein TC, Bockisch A, Antoch G. Oncologic PET/MRI, part 2: bone tumors, soft-tissue tumors, melanoma, and lymphoma. *J Nucl Med* 2012;53:1244-1252
17. Buchbender C, Heusner TA, Lauenstein TC, Bockisch A, Antoch G. Oncologic PET/MRI, part 1: tumors of the brain, head and neck, chest, abdomen, and pelvis. *J Nucl Med* 2012;53:928-938
18. Czernin J, Ta L, Herrmann K. Does PET/MR Imaging Improve Cancer Assessments? Literature Evidence from More Than 900 Patients. *J Nucl Med* 2014;55(Supplement 2):59S-62S
19. Disselhorst JA, Bezrukov I, Kolb A, Parl C, Pichler BJ. Principles of PET/MR Imaging. *J Nucl Med* 2014;55(Supplement 2):2S-10S
20. Drzezga A, Souvatzoglou M, Eiber M, Beer AJ, Fürst S, Martinez-Möller A, et al. First clinical experience with integrated whole-body PET/MR: comparison to PET/CT in patients with oncologic diagnoses. *J Nucl Med* 2012;53:845-855
21. Quick HH, von Gall C, Zeilinger M, Wiesmüller M, Braun H, Ziegler S, et al. Integrated whole-body PET/MR hybrid imaging: clinical experience. *Invest Radiol* 2013;48:280-289
22. von Schulthess GK, Veit-Haibach P. Workflow Considerations in PET/MR Imaging. *J Nucl Med* 2014;55(Supplement 2):19S-24S
23. Torigian DA, Zaidi H, Kwee TC, Saboury B, Udupa JK, Cho ZH, et al. PET/MR imaging: technical aspects and potential clinical applications. *Radiology* 2013;267:26-44
24. Vaska P, Cao T. The state of instrumentation for combined positron emission tomography and magnetic resonance imaging. *Semin Nucl Med* 2013;43:11-18
25. von Schulthess GK, Kuhn FP, Kaufmann P, Veit-Haibach P. Clinical positron emission tomography/magnetic resonance imaging applications. *Semin Nucl Med* 2013;43:3-10
26. Bailey DL. Transmission scanning in emission tomography. *Eur J Nucl Med* 1998;25:774-787
27. Zaidi H, Hasegawa B. Determination of the attenuation map in emission tomography. *J Nucl Med* 2003;44:291-315
28. Ollinger JM. Model-based scatter correction for fully 3D PET. *Phys Med Biol* 1996;41:153-176
29. Burger C, Goerres G, Schoenes S, Buck A, Lonn AH, Von Schulthess GK. PET attenuation coefficients from CT images: experimental evaluation of the transformation of CT into PET 511-keV attenuation coefficients. *Eur J Nucl Med Mol Imaging* 2002;29:922-927
30. Kinahan PE, Hasegawa BH, Beyer T. X-ray-based attenuation correction for positron emission tomography/computed tomography scanners. *Semin Nucl Med* 2003;33:166-179
31. Townsend DW. Dual-modality imaging: combining anatomy and function. *J Nucl Med* 2008;49:938-955
32. Delso G, Martinez-Möller A, Bundschuh RA, Ladebeck R, Candidus Y, Faul D, et al. Evaluation of the attenuation properties of MR equipment for its use in a whole-body PET/MR scanner. *Phys Med Biol* 2010;55:4361-4374
33. Delso G, Martinez-Möller A, Bundschuh RA, Nekolla SG, Ziegler SI. The effect of limited MR field of view in MR/PET attenuation correction. *Med Phys* 2010;37:2804-2812
34. MacDonald LR, Kohlmyer S, Liu C, Lewellen TK, Kinahan PE. Effects of MR surface coils on PET quantification. *Med Phys* 2011;38:2948-2956
35. Montandon ML, Zaidi H. Atlas-guided non-uniform attenuation correction in cerebral 3D PET imaging. *Neuroimage* 2005;25:278-286
36. Kim JS, Lee JS, Park MH, Kim KM, Oh SH, Cheon GJ, et al. Feasibility of template-guided attenuation correction in cat brain PET imaging. *Mol Imaging Biol* 2010;12:250-258
37. Berker Y, Franke J, Salomon A, Palmowski M, Donker HC, Temur Y, et al. MRI-based attenuation correction for hybrid PET/MRI systems: a 4-class tissue segmentation technique using a combined ultrashort-echo-time/Dixon MRI sequence. *J Nucl Med* 2012;53:796-804
38. Hofmann M, Steinke F, Scheel V, Charpiat G, Farquhar J, Aschoff P, et al. MRI-based attenuation correction for PET/MRI: a novel approach combining pattern recognition and atlas registration. *J Nucl Med* 2008;49:1875-1883
39. Hofmann M, Bezrukov I, Mantlik F, Aschoff P, Steinke F, Beyer T, et al. MRI-based attenuation correction for whole-body PET/MRI: quantitative evaluation of segmentation- and atlas-based methods. *J Nucl Med* 2011;52:1392-1399
40. Martinez-Möller A, Souvatzoglou M, Delso G, Bundschuh RA, Chefd'hotel C, Ziegler SI, et al. Tissue classification as a potential approach for attenuation correction in whole-body PET/MRI: evaluation with PET/CT data. *J Nucl Med* 2009;50:520-526
41. Keereman V, Fierens Y, Broux T, De Deene Y, Lonneux M, Vandenberghe S. MRI-based attenuation correction for PET/MRI using ultrashort echo time sequences. *J Nucl Med* 2010;51:812-818
42. Schulz V, Torres-Espallardo I, Renisch S, Hu Z, Ojha N, Börnert P, et al. Automatic, three-segment, MR-based attenuation correction for whole-body PET/MR data. *Eur J Nucl Med Mol Imaging* 2011;38:138-152
43. Eiber M, Martinez-Möller A, Souvatzoglou M, Holzapfel K, Pickhard A, Löffelbein D, et al. Value of a Dixon-based MR/PET attenuation correction sequence for the localization and evaluation of PET-positive lesions. *Eur J Nucl Med Mol Imaging* 2011;38:1691-1701

44. Kim JH, Lee JS, Song IC, Lee DS. Comparison of segmentation-based attenuation correction methods for PET/MRI: evaluation of bone and liver standardized uptake value with oncologic PET/CT data. *J Nucl Med* 2012;53:1878-1882
45. Eiber M, Takei T, Souvatzoglou M, Mayerhoefer ME, Fürst S, Gaertner FC, et al. Performance of whole-body integrated 18F-FDG PET/MR in comparison to PET/CT for evaluation of malignant bone lesions. *J Nucl Med* 2014;55:191-197
46. Catana C, van der Kouwe A, Benner T, Michel CJ, Hamm M, Fenchel M, et al. Toward implementing an MRI-based PET attenuation-correction method for neurologic studies on the MR-PET brain prototype. *J Nucl Med* 2010;51:1431-1438
47. Aitken AP, Giese D, Tsoumpas C, Schleyer P, Kozerke S, Prieto C, et al. Improved UTE-based attenuation correction for cranial PET-MR using dynamic magnetic field monitoring. *Med Phys* 2014;41:012302
48. Dickson JC, O'Meara C, Barnes A. A comparison of CT- and MR-based attenuation correction in neurological PET. *Eur J Nucl Med Mol Imaging* 2014;41:1176-1189
49. Nuyts J, Dupont P, Stroobants S, Benninck R, Mortelmans L, Suetens P. Simultaneous maximum a posteriori reconstruction of attenuation and activity distributions from emission sinograms. *IEEE Trans Med Imaging* 1999;18:393-403
50. Defrise M, Rezaei A, Nuyts J. Time-of-flight PET data determine the attenuation sinogram up to a constant. *Phys Med Biol* 2012;57:885-899
51. Conti M. Why is TOF PET reconstruction a more robust method in the presence of inconsistent data? *Phys Med Biol* 2011;56:155-168
52. Keereman V, Mollet P, Berker Y, Schulz V, Vandenberghe S. Challenges and current methods for attenuation correction in PET/MR. *MAGMA* 2013;26:81-98
53. Weber WA. PET/MR Imaging: A Critical Appraisal. *J Nucl Med* 2014;55(Supplement 2):56S-58S
54. Rauscher I, Eiber M, Souvatzoglou M, Schwaiger M, Beer AJ. PET/MR in Oncology: Non-18F-FDG Tracers for Routine Applications. *J Nucl Med* 2014;55(Supplement 2):25S-31S
55. Liu X, Yetik IS. Automated prostate cancer localization without the need for peripheral zone extraction using multiparametric MRI. *Med Phys* 2011;38:2986-2994
56. Wehrl HF, Wiehr S, Divine MR, Gatidis S, Gullberg GT, Maier FC, et al. Preclinical and Translational PET/MR Imaging. *J Nucl Med* 2014;55(Supplement 2):11S-18S
57. Histed SN, Lindenberg ML, Mena E, Turkbey B, Choyke PL, Kurdziel KA. Review of functional/anatomical imaging in oncology. *Nucl Med Commun* 2012;33:349-361
58. Filss CP, Galldiks N, Stoffels G, Sabel M, Wittsack HJ, Turowski B, et al. Comparison of 18F-FET PET and perfusion-weighted MR imaging: a PET/MR imaging hybrid study in patients with brain tumors. *J Nucl Med* 2014;55:540-545
59. Kuhn FP, Hüllner M, Mader CE, Kastrinidis N, Huber GF, von Schulthess GK, et al. Contrast-enhanced PET/MR imaging versus contrast-enhanced PET/CT in head and neck cancer: how much MR information is needed? *J Nucl Med* 2014;55:551-558
60. Platzek I, Beuthien-Baumann B, Schneider M, Gudziol V, Kitzler HH, Maus J, et al. FDG PET/MR for lymph node staging in head and neck cancer. *Eur J Radiol* 2014;83:1163-1168
61. Platzek I, Beuthien-Baumann B, Schneider M, Gudziol V, Langner J, Schramm G, et al. PET/MRI in head and neck cancer: initial experience. *Eur J Nucl Med Mol Imaging* 2013;40:6-11
62. Donati OF, Hany TF, Reiner CS, von Schulthess GK, Marincek B, Seifert B, et al. Value of retrospective fusion of PET and MR images in detection of hepatic metastases: comparison with 18F-FDG PET/CT and Gd-EOB-DTPA-enhanced MRI. *J Nucl Med* 2010;51:692-699
63. Sun H, Xin J, Zhang S, Guo Q, Lu Y, Zhai W, et al. Anatomical and functional volume concordance between FDG PET, and T2 and diffusion-weighted MRI for cervical cancer: a hybrid PET/MR study. *Eur J Nucl Med Mol Imaging* 2014;41:898-905
64. Souvatzoglou M, Eiber M, Takei T, Fürst S, Maurer T, Gaertner F, et al. Comparison of integrated whole-body [11C]choline PET/MR with PET/CT in patients with prostate cancer. *Eur J Nucl Med Mol Imaging* 2013;40:1486-1499
65. Gaertner FC, Beer AJ, Souvatzoglou M, Eiber M, Fürst S, Ziegler SI, et al. Evaluation of feasibility and image quality of 68Ga-DOTATOC positron emission tomography/magnetic resonance in comparison with positron emission tomography/computed tomography in patients with neuroendocrine tumors. *Invest Radiol* 2013;48:263-272
66. Somer EJ, Marsden PK, Benatar NA, Goodey J, O'Doherty MJ, Smith MA. PET-MR image fusion in soft tissue sarcoma: accuracy, reliability and practicality of interactive point-based and automated mutual information techniques. *Eur J Nucl Med Mol Imaging* 2003;30:54-62
67. Park H, Wood D, Hussain H, Meyer CR, Shah RB, Johnson TD, et al. Introducing parametric fusion PET/MRI of primary prostate cancer. *J Nucl Med* 2012;53:546-551
68. Jambor I, Borra R, Kemppainen J, Lepomäki V, Parkkola R, Dean K, et al. Improved detection of localized prostate cancer using co-registered MRI and 11C-acetate PET/CT. *Eur J Radiol* 2012;81:2966-2972
69. Takei T, Souvatzoglou M, Beer AJ, Drzezga A, Ziegler S, Rummeny EJ, et al. A case of multimodality multiparametric 11C-choline PET/MR for biopsy targeting in prior biopsy-negative primary prostate cancer. *Clin Nucl Med* 2012;37:918-919
70. Afshar-Oromieh A, Haberkorn U, Schlemmer HP, Fenchel M, Eder M, Eisenhut M, et al. Comparison of PET/CT and PET/MRI hybrid systems using a 68Ga-labelled PSMA ligand for the diagnosis of recurrent prostate cancer: initial experience. *Eur J Nucl Med Mol Imaging* 2014;41:887-897
71. Schuler MK, Richter S, Beuthien-Baumann B, Platzek I, Kotzerke J, van den Hoff J, et al. PET/MRI Imaging in High-Risk Sarcoma: First Findings and Solving Clinical Problems. *Case Rep Oncol Med* 2013;2013:793927
72. Gaeta CM, Vercher-Conejero JL, Sher AC, Kohan A, Rubbert C, Avril N. Recurrent and metastatic breast cancer PET, PET/CT,

PET/MRI: FDG and new biomarkers. *Q J Nucl Med Mol Imaging* 2013;57:352-366
73. Kubiessa K, Purz S, Gawlitza M, Kühn A, Fuchs J, Steinhoff KG, et al. Initial clinical results of simultaneous 18F-FDG PET/MRI in comparison to 18F-FDG PET/CT in patients with head and neck cancer. *Eur J Nucl Med Mol Imaging* 2014;41:639-648
74. Collins CD. PET/CT in oncology: for which tumours is it the reference standard? *Cancer Imaging* 2007;7 Spec No A:S77-S87
75. Kohan AA, Kolthammer JA, Vercher-Conejero JL, Rubbert C, Partovi S, Jones R, et al. N staging of lung cancer patients with PET/MRI using a three-segment model attenuation correction algorithm: initial experience. *Eur Radiol* 2013;23:3161-3169
76. Thorek DL, Ulmert D, Diop NF, Lupu ME, Doran MG, Huang R, et al. Non-invasive mapping of deep-tissue lymph nodes in live animals using a multimodal PET/MRI nanoparticle. *Nat Commun* 2014;5:3097
77. Antoch G, Vogt FM, Freudenberg LS, Nazaradeh F, Goehde SC, Barkhausen J, et al. Whole-body dual-modality PET/CT and whole-body MRI for tumor staging in oncology. *JAMA* 2003;290:3199-3206
78. Schmidt GP, Schoenberg SO, Schmid R, Stahl R, Tiling R, Becker CR, et al. Screening for bone metastases: whole-body MRI using a 32-channel system versus dual-modality PET-CT. *Eur Radiol* 2007;17:939-949
79. Ohno Y, Koyama H, Onishi Y, Takenaka D, Nogami M, Yoshikawa T, et al. Non-small cell lung cancer: whole-body MR examination for M-stage assessment--utility for whole-body diffusion-weighted imaging compared with integrated FDG PET/CT. *Radiology* 2008;248:643-654
80. Coenegrachts K, De Geeter F, ter Beek L, Walgraeve N, Bipat S, Stoker J, et al. Comparison of MRI (including SS SE-EPI and SPIO-enhanced MRI) and FDG-PET/CT for the detection of colorectal liver metastases. *Eur Radiol* 2009;19:370-379
81. Takenaka D, Ohno Y, Matsumoto K, Aoyama N, Onishi Y, Koyama H, et al. Detection of bone metastases in non-small cell lung cancer patients: comparison of whole-body diffusion-weighted imaging (DWI), whole-body MR imaging without and with DWI, whole-body FDG-PET/CT, and bone scintigraphy. *J Magn Reson Imaging* 2009;30:298-308
82. Niekel MC, Bipat S, Stoker J. Diagnostic imaging of colorectal liver metastases with CT, MR imaging, FDG PET, and/or FDG PET/CT: a meta-analysis of prospective studies including patients who have not previously undergone treatment. *Radiology* 2010;257:674-684
83. Yong TW, Yuan ZZ, Jun Z, Lin Z, He WZ, Juanqi Z. Sensitivity of PET/MR images in liver metastases from colorectal carcinoma. *Hell J Nucl Med* 2011;14:264-268
84. Kwee SA, Ko JP, Jiang CS, Watters MR, Coel MN. Solitary brain lesions enhancing at MR imaging: evaluation with fluorine 18 fluorocholine PET. *Radiology* 2007;244:557-565
85. Yoon SH, Goo JM, Lee SM, Park CM, Seo HJ, Cheon GJ. Positron emission tomography/magnetic resonance imaging evaluation of lung cancer: current status and future prospects. *J Thorac Imaging* 2014;29:4-16
86. Chandarana H, Heacock L, Rakheja R, DeMello LR, Bonavita J, Block TK, et al. Pulmonary nodules in patients with primary malignancy: comparison of hybrid PET/MR and PET/CT imaging. *Radiology* 2013;268:874-881
87. Wahl RL, Jacene H, Kasamon Y, Lodge MA. From RECIST to PERCIST: Evolving Considerations for PET response criteria in solid tumors. *J Nucl Med* 2009;50 Suppl 1:122S-150S
88. Heijmen L, Verstappen MC, Ter Voert EE, Punt CJ, Oyen WJ, de Geus-Oei LF, et al. Tumour response prediction by diffusion-weighted MR imaging: ready for clinical use? *Crit Rev Oncol Hematol* 2012;83:194-207
89. Afaq A, Andreou A, Koh DM. Diffusion-weighted magnetic resonance imaging for tumour response assessment: why, when and how? *Cancer Imaging* 2010;10 Spec no A:S179-S188
90. Platzek I, Beuthien-Baumann B, Langner J, Popp M, Schramm G, Ordemann R, et al. PET/MR for therapy response evaluation in malignant lymphoma: initial experience. *MAGMA* 2013;26:49-55
91. Purz S, Sabri O, Viehweger A, Barthel H, Kluge R, Sorge I, et al. Potential Pediatric Applications of PET/MR. *J Nucl Med* 2014;55(Supplement 2):32S-39S
92. Hirsch FW, Sattler B, Sorge I, Kurch L, Viehweger A, Ritter L, et al. PET/MR in children. Initial clinical experience in paediatric oncology using an integrated PET/MR scanner. *Pediatr Radiol* 2013;43:860-875
93. Punwani S, Taylor SA, Bainbridge A, Prakash V, Bandula S, De Vita E, et al. Pediatric and adolescent lymphoma: comparison of whole-body STIR half-Fourier RARE MR imaging with an enhanced PET/CT reference for initial staging. *Radiology* 2010;255:182-190
94. Lin C, Luciani A, Itti E, El-Gnaoui T, Vignaud A, Beaussart P, et al. Whole-body diffusion-weighted magnetic resonance imaging with apparent diffusion coefficient mapping for staging patients with diffuse large B-cell lymphoma. *Eur Radiol* 2010;20:2027-2038
95. Baur A, Stäbler A, Nagel D, Lamerz R, Bartl R, Hiller E, et al. Magnetic resonance imaging as a supplement for the clinical staging system of Durie and Salmon? *Cancer* 2002;95:1334-1345
96. Ripa RS, Knudsen A, Hag AM, Lebech AM, Loft A, Keller SH, et al. Feasibility of simultaneous PET/MR of the carotid artery: first clinical experience and comparison to PET/CT. *Am J Nucl Med Mol Imaging* 2013;3:361-371
97. Nappi C, El Fakhri G. State of the Art in Cardiac Hybrid Technology: PET/MR. *Curr Cardiovasc Imaging Rep* 2013;6:338-345
98. Nensa F, Poeppel TD, Beiderwellen K, Schelhorn J, Mahabadi AA, Erbel R, et al. Hybrid PET/MR imaging of the heart: feasibility and initial results. *Radiology* 2013;268:366-373
99. Rischpler C, Nekolla SG, Dregely I, Schwaiger M. Hybrid PET/MR imaging of the heart: potential, initial experiences, and future prospects. *J Nucl Med* 2013;54:402-415
100. Rischpler C, Nekolla SG, Beer AJ. PET/MR imaging of

atherosclerosis: initial experience and outlook. *Am J Nucl Med Mol Imaging* 2013;3:393-396
101. Neuner I, Kaffanke JB, Langen KJ, Kops ER, Tellmann L, Stoffels G, et al. Multimodal imaging utilising integrated MR-PET for human brain tumour assessment. *Eur Radiol* 2012;22:2568-2580
102. Heiss WD. The potential of PET/MR for brain imaging. *Eur J Nucl Med Mol Imaging* 2009;36 Suppl 1:S105-S112
103. Leibfarth S, Mönnich D, Welz S, Siegel C, Schwenzer N, Schmidt H, et al. A strategy for multimodal deformable image registration to integrate PET/MR into radiotherapy treatment planning. *Acta Oncol* 2013;52:1353-1359
104. von Schulthess GK. Why buy a PET/MR for high end research? *J Magn Reson Imaging* 2014;40:283-284
105. Boss A, Bisdas S, Kolb A, Hofmann M, Ernemann U, Claussen CD, et al. Hybrid PET/MRI of intracranial masses: initial experiences and comparison to PET/CT. *J Nucl Med* 2010;51:1198-1205
106. Schwenzer NF, Stegger L, Bisdas S, Schraml C, Kolb A, Boss A, et al. Simultaneous PET/MR imaging in a human brain PET/MR system in 50 patients--current state of image quality. *Eur J Radiol* 2012;81:3472-3478
107. Boss A, Kolb A, Hofmann M, Bisdas S, Nägele T, Ernemann U, et al. Diffusion tensor imaging in a human PET/MR hybrid system. *Invest Radiol* 2010;45:270-274